ION TUNING WATERFLOODING IN LOW PERMEABILITY SANDSTONE: COREFLOODING EXPERIMENTS AND INTERPRETATION BY THERMODYNAMICS AND SIMULATION

Quan Xie; Desheng Ma; Qingjie Liu; Weifeng Lv
Research Institute of Petroleum Exploration and Development of CNPC

This paper was prepared for presentation at the International Symposium of the Society of Core Analysts held in St. John's Newfoundland and Labrador, Canada, 16-21 August, 2015

ABSTRACT

In recent years, ions tuning water flooding (ITWF) has been a promising technique to recover oil in sandstone reservoirs. In view of research results for the last decade, it is acknowledged that substantial oil recovery beyond conventional waterflooding from sandstone is wettability alteration. However, the major contributor to wettability alteration is still uncertain. Therefore, this paper investigates this major mechanism and shows how it is due to involved in the process of IOR. Rock and oil surface chemistry were tested to explain the influence of zeta potential on the disjoining pressure. Coreflood experiments with permeability less than 1mD were performed with two different brines. Moreover, the impact of different wettabilities ranging from strong water- to slight water -wet on ITWF recovery was investigated with combination of thermodynamic theory and corefloods experiments. Relative permeability curves were obtained by history matching the corefloods experiments for both oil-wet and water-wet cores with consideration of salinity effect. Thermodynamics of wettability by ion tuning waterflooding was analyzed to characterize the surface forces between the surfaces of oil/water and water/rock.

Zeta potential results showed that decreasing divalent cations and salinity makes the electrical charges at both oil/brine and brine/rock interfaces become strongly negative, which results in elevation of the repulsive forces between oil and rock, and as a result the rock turns more water-wet, which was confirmed by thermodynamics characterization. Coreflooding experiments showed that a high potential in oil-wet reservoirs can be achieved by ion tuning waterflooding due to the double layer expansion. The relative permeability curves obtained by history matching showed that ITW improves oil recovery by accelerating oil production (relative perm changes) and reducing residual oil saturation in oil-wet rock but not in water-wet rock. Thermodynamics of wettability analysis indicated that the mechanism of ion tuning waterflooding can be interpreted by disjoining pressure calculation. These findings can help in composition design of ion tuning water to maintain higher potential to recover oil in oil field.

INTRODUCTION

Waterflooding technology has been the most successful approach to improve oil recovery. The key point to reach this success of waterflooding is that the differential pressure can be formed by the water injection which is necessary to displace oil out of formation. And also, waterflooding involves much lower cost investment and convenient operation. However, it was found that water chemistry and salinity level have a significant influence on oil recovery from the experiment in the laboratory and field trials [1, 2]. In recent years, several mechanisms were proposed to account how the ions tuning waterflood to recover additional oil. (1) Fines migration and clays swelling caused by ions tuning waterflood are the main mechanism of improved oil recovery [3, 4]. (2)Multi-component ionic exchange between the rock minerals and the injected brine was proposed to be as the major mechanism to enhance oil recovery [5, 6] . (3) Expansion of the double layer to be as the dominant mechanism of oil recovery improvement[7]. The general agreement among researchers is that low salinity waterflooding cause reservoirs become more water-wet [1]. The general agreement among researchers is that low salinity waterflooding cause reservoirs become more water-wet. The main objectives of this work are (1) to examine the performance of LSW in sandstone rocks with different wettability, and investigate the role of salinity and brine composition on the performance of LSW on the secondary and tertiary recovery modes. (2) To derive the relative permeability curves from corefloods experiments to better understand the LSW performance in different wettability reservoirs. (3)Moreover, in order to have deeper understanding the mechanism of the low salinity EOR-effect, the thermodynamics of wettability was analyzed with investigation of surface chemistry of interfaces of oil/water and water/rock.

EXPERIMENTAL

Fluids

In order to investigate the impact of the rock wettability on the low salinity EOR-effect, the crude oil from the Changqing Oil Field was used in zeta potential test and corefloods experiments. The ingredients of the experimental oil from Changqing Oilfield were shown in Table 1. The experimental oil was rich in aromatic hydrocarbon and asphaltic bitumen, the main source of the carboxy and amino groups. The density of oil sample was 0.81 g/cm^3 with viscosity at 9.0 cp at temperature of 65℃.

Two different brines were used in the corefloods and zeta potential tests; the one was synthetic brine according to the formation brine formula. Another is the low salinity brine, which was diluted 10 times by adding deionized water. The composition of the formation brine and LSW were given in Table 2. The total salinity of the brine water was 57114mg/L with the concentration of Ca^{2+} and Mg^{2+} at 2460mg/L and 317mg/L, respectively.

Mineralogy of Reservoir Cores

The core plugs for coreflood experiments were extracted from the Chang Qing oilfield and outcrop in Chang Qing. The content of clays was analyzed by X-ray test to unveil the importance of the clays on the low salinity EOR-effect in low permeability reservoirs, as shown in Table 3. The reservoir cores were rich in clays, which was more than 23% in total. 92.8% quartz and 4.2% clay content were observed from the outcrop core plugs. The composition of the outcrop indicated that it could be water-wet because of high content of quartz in the rock.

Table 1 Ingredients of the oil sample from Changqing Oilfield

Ingredients	Saturated hydrocarbon	Aromatic hydrocarbon	Non-hydrocarbon	Asphaltic bitumen
wt%	65.05	23.30	6.68	4.97

Table 2 Composition of the formation brine and low salinity water (LSW)

Brines	Ingredients（mg/l）					TDS (mg/l)
	K^++Na^+	Ca^{2+}	Mg^{2+}	HCO^{3-}	Cl^-	
Formation brine/HSW	19249	2460	317	308	34780	57114
Ion tuning water/ITW	1924.9	246	31.7	30.8	3478	5711.4

Table 3 Mineralogy of the experimental core plugs

Sample	Relative content of clay minerals（%）				Mineral types and content（%）				Total clay minerals（%）
	Mix	I	K	C	quartz	potassium feldspar	plagioclase	calcite	
Outcrop	25	25	5	45	92.8	/	1.4	1.6	4.2
Reservoir core	32	12	28	28	43.2	11.9	20.9	0.4	23.6

Note: I-illite, K-Kaolinite, C-Chlorite, Mix-Illite/Smectite

Zeta Potential

Zeta potential technique was applied to understand the relation between electric double layer and wettability regarding the charges at interfaces of oil/brine and solids/brine. Rock wettability is closely related to the thickness of water film between rock surface and crude oil, which depends on the electrical double layer repulsion and Van der Waals force. Wettability of the rock will be determined by the stability of the water film which is bounded by the interfaces of oil/brine and solid/brine [8, 9]. An unstable water film, or thin water film, may cause the wettability preferential to be oil-wet. Therefore, injection water with different ions types and concentration will trigger the alternation of the surface charges at both interfaces – oil/brine and solids/brine. Then, oil film may detach from the pore wall by increase of electrical double layer repulsion and the oil recovery will be improved.

In this study, the protocol of zeta potential tests was shown in a published paper [10]. Results of zeta potential of oil/brine and solid/brine interfaces were given to investigate the influence of the double layer expansion on low salinity EOR-effect in oil-wet and water-wet core plugs, as shown in Figure 1. The pHs of the two different brines with adding powders of rocks and crude oil were measured after equilibrium, as shown in Figure 2, due to the zeta potential magnitude varying with pH value.

Figure 1 shows that LSW resulted in stronger negative charges at the surface of reservoir rock/brine, outcrop rock/brine and crude oil/brine. This is consistent with most of the zeta potential test for low salinity waterflooding. However, LSW increased the negative surface charges at interface of outcrop rock/brine, compared to HSW, This result shows that the mineral and clay content of the rock is closely related to the zeta potential for certain brine. Basically, the larger the clay content, the more sensitive the zeta potential to the brine salinity, regarding to the variation of the brine salinity. Zeta potential of reservoir rock with LSW and HSW also proves that salinity strongly impact on the electric surface charge at the oil/brine and rock/brine interfaces [7].

Figure 2 shows that pH of outcrop rock/HSW and outcrop rock/LSW was about 7.0 and 7.5, respectively. However, the pH of reservoir rock/HSW and reservoir rock/LSW was about 6.2 and 8.0, respectively. The pH increase in the LSW compared with HSW was interpreted by the chemical equilibrium given as below moving to the right because of the low salinity water invasion [11].

$$NaAlSi_3O_8 + H_2O \longleftrightarrow HAlSi_3O_8 + Na^+ + OH^- \quad (1)$$

$$Clay\text{-}Ca^{2+} + H_2O \longleftrightarrow Clay\text{-}H^+ + Ca^{2+} + OH^- \quad (2)$$

$$R\text{-}COOH \longleftrightarrow R\text{-}COO^- + H^+ \quad (3)$$

Chemical Equation (1) and (2) also indicate that the higher pH increase could be observed if the rock is rich in clays and $NaAlSi_3O_8$, which is consistent with the rock mineralogy, as shown in Table 3.

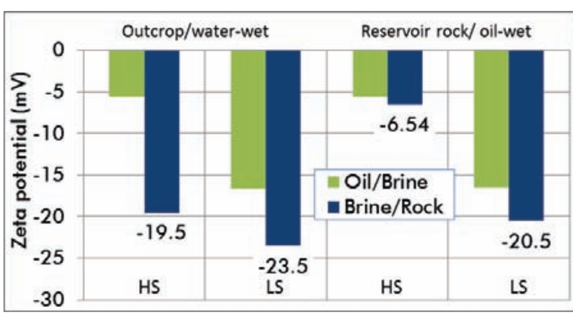

Figure 1 zeta potential results of oil/brine and solid/brine interfaces

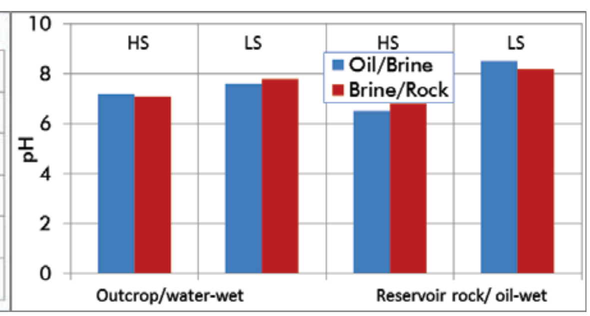

Figure 2 pHs of the two different brines with adding powers of rocks and crude oil

Wettability Measurement

The Amott test is one of the most widely used empirical wettability measurements for reservoir cores in petroleum engineering. Wettabilities of preserved core plugs were measured with the improved Amott water index method which is slightly different from the conventional procedure. This Amott water index approach combines spontaneous imbibition and forced imbibition processes. The experimental procedures adopted in this paper were introduced in a literature [12]. Crude oil from Changqing oil field was used to desaturate the core plugs, then they were put into an oven at 65°C for aging four weeks to restore the wettability.

The magnitude of I_w is from 0 to 1. The higher I_w , the more water-wet. The results of wettability test were given in Table 4, which shows that the outcrop core plug OC-1# was strongly water-wet and reservoir rock RC-1# was slightly water-wet. The two types of the core plugs with different wettability were used to conduct corefloods experiments for investigation of LSW performance, which was discussed later in this study.

Table 4 Physical properties of cores and the Amott test results

Core sample	Core properties					Amott test		
	Diameter (cm)	Length (cm)	Pore volume (mL)	Porosity (%)	Swi (%)	Sws (%)	Sor (%)	Iw
OC-1#	2.5	7.15	4.60	13.1	26.8	60.2	64.9	0.88
RC-1#	2.5	7.2	4.45	12.6	31.1	41.2	54.8	0.43

S_{wi}, initial water saturation; S_{ws}, water saturation after spontaneous imbibition of water; S_{or}, residual oil saturation after forced displacement.

COREFLOODING EXPERIMENTS AND SIMULATIONS

Coreflooding Experiments Protocols

In order to investigate the influence of wettability on low salinity water EOR effect, corefloods experiments were executed by using two reservoir cores and two cores from the outcrop. For each type of wettability, low salinity water was used under secondary and tertiary mode with the core plugs, which were initially saturated by formation brine. Due to the small changes in saturation followed by low salinity waterflooding under tertiary mode, unsteady state (USS) under tertiary and secondary by using low salinity water flooding were history matched to derive the low salinity water relative permeability curves [13]. All of the coreflood experiments were conducted at 65°C. The brine permeability of the experimental cores was lower than 1 mD, as shown in Table 5 and Table 6. The injection rate was 0.025ml/min. The procedures of corefloods experiments and set-up were selected from literature [10].

Methodology of History Matching in Core Scale

A one-dimensional homogeneous permeability core model was established to simulate the characteristics of oil recovery by forced imbibition with the finite difference simulator ECLIPSE 100. There were 22 equal-sized grid blocks in the core model. The first grid which was located at the upstream of the core was saturated with 100% formation brine with 100% porosity, but 1000 D permeability was assigned to simulate the experimental injection. The last grid at the outlet of the core was saturated 100% oil with 0.001% porosity and 1000 D permeability since at beginning of the forced imbibition the outlet of the core was filled with 100% experimental oil. Porosity and permeability of each of the cells except of inlet and outlet cells was assumed to be equal. Porosity was obtained by Helium Porsimeter (PHI-220) under room temperature and permeability was measured through coreflooding experiment by injection of formation brine with saturated core plugs. The summary of composite core model for experiments and simulation model were given in Table 5.

According to the waterflooding simulation through ECLIPSE 100, the significant parameters dominating oil recovery and differential pressure by forced imbibition are the capillary pressure and relative permeability curves. The functional forms in Eqs. (4)-(6) are

$$k_{rw} = k_{rw}^{*}\left(\frac{S_w - S_{wi}}{1 - S_{or} - S_{wi}}\right)^{n_{rw}} \tag{4}$$

$$k_{ro} = k_{ro}^{*}\left(1 - \frac{S_w - S_{wi}}{1 - S_{or} - S_{wi}}\right)^{n_{r0}} \tag{5}$$

$$P^{c} = \sqrt{\frac{\phi}{k}}\sigma J^{*}\left(1 - \frac{S_w - S_{wi}}{S_{w0} - S_{wi}}\right)^{n_{pc}} \tag{6}$$

Where k_{rw} is the water relative permeability and k_{ro} is the oil relative permeability. P_c is the capillary pressure, and S is the phase saturation. The subscripts w, w_i and w_o represent water, initial water, residual oil at water saturation where the capillary pressure is equal to zero, respectively. The superscript $*$ denotes the end-point.

Table 5 Summary of composite core model for four experiments

Properties	Outcrop		Reservoir cores	
Samples	OC-2#	OC-3#	RC-2#	RC-3#
Flooding sequences	HS + LS	LS	HS + LS	LS
Porosity	0.136	0.140	0.129	0.123
Kw (mD)	0.331	0.340	0.92	0.82
Pore volume (cm^3)	4.770	4.810	4.3665	4.2029
Length (cm)	7.115	6.990	6.867	6.927
Diameter (cm)	2.504	2.504	2.5059	2.5068
Bulk volume (cm^3)	35.03	34.37	33.849	34.170
Cross sectional area (cm^2)	4.924	4.917	4.9292	4.9328
Grid block dimensions	20 × 1 × 1	20 × 1 × 1	20 × 1 × 1	20 × 1 × 1
Width (cm)	0.35575	0.34955	0.34335	0.34635
Height (cm)	2.219009	2.217431	2.2202	2.2210

Table 6 Summary of composite core model for four experiments

Properties	Outcrop		Reservoir cores	
Samples	OC-2#	OC-3#	RC-2#	RC-3#
Flooding sequences	HS + LS	LS	HS + LS	LS
no	2.2	2.1	5.2	3.2
nw	6.2	6.3	3.1	4.8
Krw(Sorw)	0.09	0.09	0.35	0.2
Kro(Swc)	1.0	1.0	1.0	1.0
Sorw	0.363(HS)/0.331 (LS)	0.339	0.412	0.382
Swc	0.268	0.291	0.322	0.315

Effect of Low Salinity Waterflooding on Reservoir Cores

Low salinity EOR-effect has been closely related to the change of wettability of reservoirs according to studies during the past more than a decade. However, the influence of the wettability in low permeability reservoirs on the low salinity waterflooding is rarely reported with combination of corefloods experiments, core-scale history matching. Therefore, this paper unveils the deeper understanding of low salinity EOR-effect through corefloods experiments on various wettability cores, core-scale history matching and thermodynamics analysis, which will be discussed at the last part of this study. Two reservoir cores, either flooded by low salinity water under secondary or tertiary mode, were implemented to conduct coreflooding. Both oil recovery and differential pressure by high and low salinity waterflooding were successfully history matched to derive the relative permeability curves, as shown in Figure 3, Figure 4 and Figure 5.

Figure 3 and Figure 4 show that low salinity waterflooding can improve oil recovery about 10% of OOIP under both secondary and tertiary mode, compared with high salinity waterflooding. Both of the Figures also indicate that the low salinity water can accelerate the oil production rate and reduce the residual oil saturation, with comparison of the high salinity waterflooding. This coreflood phenomenon proves that the great potential of low salinity waterflood effect may be observed as the reservoir is slightly water wet. This difference between LSWF and HSWF might be interpreted as a change in reservoir's wettability with invasion of low salinity brine. This can be proved by relative permeability curves derived by core-scale history matching, which was discussed below. In conclusion, low salinity water can accelerate the oil production rate and decelerate the water production rate by reduction of the residual oil saturation in reservoirs.

Low salinity EOR-effect on reservoir cores were also observed by the relative permeability curves (Figure 5), which were derived from the core-scale history matching by ECLIPSE 100 with low salinity model. Figure 5 shows that relative permeability curves for low salinity waterfood moves toward to the right, which might be interpreted as the transition of the wettability towards more water-wet. The capillary pressure curves were not shown here, due to the insensitivity to the core-scale history matching in the low permeability corefloods. As the corefloods experiments shown, the differential pressure was 1 to 2 MPa, which was much higher than the capillary pressure.

The incremental oil recovery by LSW compared to HSW could be attributed to the expansion of the electric double layer, which is caused by LSW as a result of increasing the magnitude of the negative electric charge at the interfaces of oil/brine and rock/brine. HSW caused weak surface charges at both oil/brine and rock/brine interfaces. However, more negative charges at oil/brine and brine/rock were generated by LSW. According to the theoretical calculation of thermodynamics, which will be discussed at the last part of this study, more negative charges at the interfaces of oil/LSW and LSW/rock and corresponding increase of the repulsive forces might detach the oil film from the rock surface.

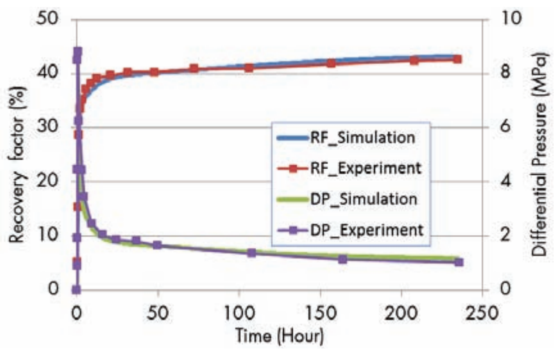

Figure 3 Low salinity waterflooding under secondary mode with the core from the reservoir (slightly water-wet)

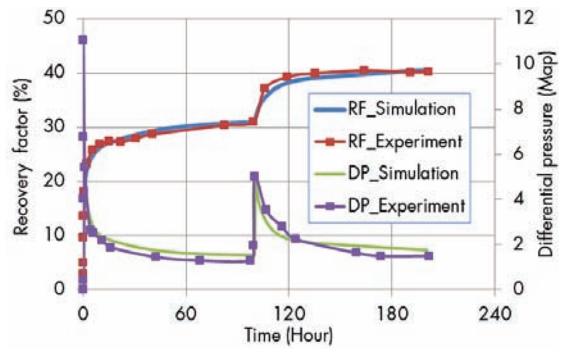

Figure 4 Low salinity waterflooding under tertiary mode with the core from the reservoir (slightly water-wet)

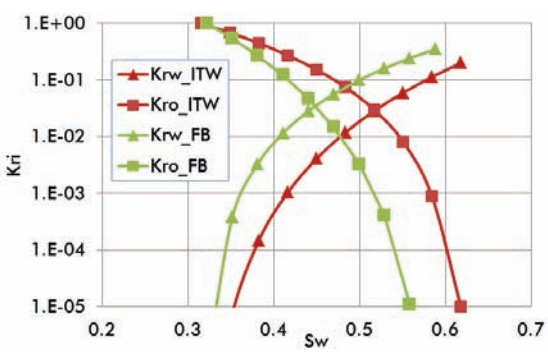

Figure 5 Relative permeability curves of low salinity and high salinity waterflooding (reservoir cores)

Effect of Low salinity Waterflooding on Water-wet Reservoir

According the the literature, the low salinity EOR-effect was rarely observed in the water-wet reservoirs. In order to further confirm and reveal the mechanism behind his phenomenon, two core plugs extracted from the outcrop were used to perform coreflooding with low salinity water, either in secondary mode or tertiary mode (Figure 6 and Figure 7). The experimental oil was from the Changqing Oil Field and the core plugs were put into the oven with 65^{o}C for four weeks after the cores desaturated with experimental oil to restore the wettability. Additionally, the corefloods experiments were successfully history matched to acquire the relative permeability curves, as shown in Figure 8.

Figure 6 and Figure 7 show that slight low salinity EOR-Effect was observed from low salinity waterflooding under secondary and tertiary mode. Figure 6 presents that 50.5% oil recovery of OOIP was accumulated by low salinity waterflooding. Figure 7 also shows that 50.0% oil recovery of OOIP was obtained by the high salinity waterflooding under secondary mode. Additional 3.4% oil recovery of OOIP was observed by low salinity waterflooding under tertiary mode. Relative permeability curves illustrates that the wettability of the outcrop was preferential to water-wet and minor wettability change during the low salinity waterflood was observed (Figure 8). Coreflooding experiments, by using water-wet outcrop core plugs, verified that low salinity effect may not work in the water-wet reservoirs. Moreover, with comparison of Figure 4 and Figure 7, piston-like displacement was found for high salinity water flooding as the core was water-wet, while the oil was produced over much longer periods for high salinity water flooding as the core was slightly water wet. This could be due to the more favorable mobility ratio formed by the low salinity water flooding in the reservoir [14].

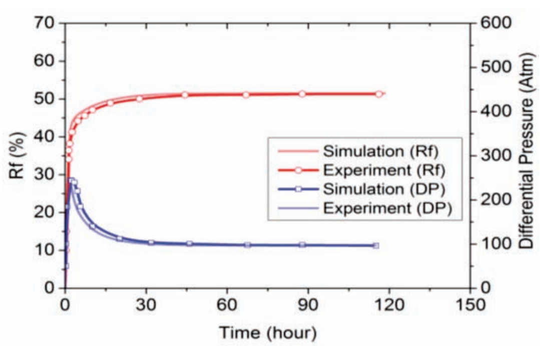

Figure 6 Low salinity waterflooding under secondary mode with the core from outcrop (water-wet)

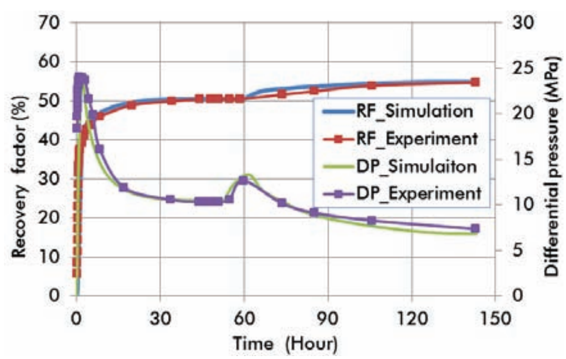

Figure 7 Low salinity waterflooding under tertiary mode with the core from outcrop (water-wet)

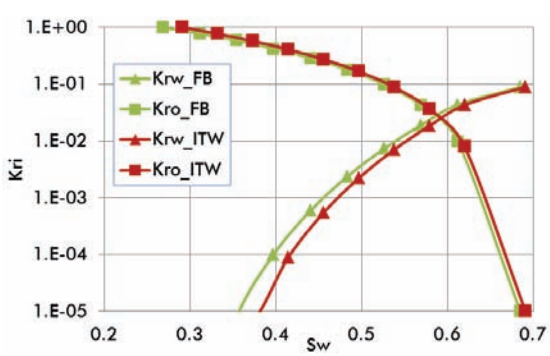

Figure 8 Relative permeability curves of low salinity and high salinity waterflooding (outcrop, water-wet)

THERMODYNAMICS ANALYSIS

Thermodynamics Background

Hirasaki has investigated the thermodynamics of the thin films to determine the interdependence of spreading, contact angle and capillary pressure using the DLVO theory and Laplace-Young Equation [8]. The intermolecular forces comprise of the van der Waals, electrical and structural forces.

$$\Pi_{Total} = \Pi_{Van-der-Waals} + \Pi_{electrical} + \Pi_{structural} \tag{7}$$

Where, Π_{Total} is the disjoining pressure of the specific intermolecular interactions which reflects the interactive forces between the interface of water/oil and water/rock. In this study, dielectric constants for each of medium were tested through N5224A microwave network analyzer, 2.84×10^{-21}J was used as the Hamaker constant for outcrop/brine/oil system, 3.70×10^{-21}J was used for reservoir rock/brine/oil system, A brief introduction of the forces and calculation procedures are presented in literatures [15].

Thermodynamic Calculation on Reservoir Cores and Outcrop

According to the theoretical model, structural forces were assumed to be as same with respect to the variation of molarity and zeta potential. Therefore, the variations of disjoining pressure could be explained by only considering the electrostatic interactions and Van der Waals forces, calculated with consideration of mineralogy difference. With combination of zeta potential measurement and composition of the brines, the disjoining pressure versus water film thickness was calculated (Figure 9) to unveil the deeper mechanism behind the low salinity waterflooding.

Figure 9 shows that the formation brine resulted in attractive force between the interface of oil/brine and interface of brine/rock in the slightly water wet rock. However, the repulsive force between the interfaces of oil/brine/rock was formed by low salinity water due to the low salinity and highly negative zeta potential for both interfaces of oil/water and water/rock. Figure 9 also shows that the water film was thicker in high salinity brine, compared with the low salinity brine due to the double layer expansion. Thicker water film indicates that the rock surface is preferential to water-wet with lower surface energy with presence of low salinity brine. Moreover, the thermodynamic isothermal calculation is consistent with the results of wettability test and corefloods experiments for the reservoir rocks.

Figure 10 illustrates that both formation brine and low salinity water causes the repulsive force between the interfaces of oil/water and water/rock in the water-wet rock. This also fits the results of wettability test and corefloods experiments for the water-wet outcrop rocks. Even though the thicker water film and repulsive force were formed as result of double layer expansion in low salinity brine, repulsive force still remained in the formation brine with thinner water film. The thermodynamic analysis for water-wet rock discloses that low salinity EOR-effect would not be observed in the water-wet reservoirs. Therefore, the conclusions can be drawn are: firstly, the thermodynamic isothermal can be applied to unveil the mechanism behind the low salinity EOR-effect. Secondly, it can be used to screen the candidate reservoirs for low salinity waterflooding. Thirdly, composition of injection brine can be manipulated by the calculation of thermodynamics.

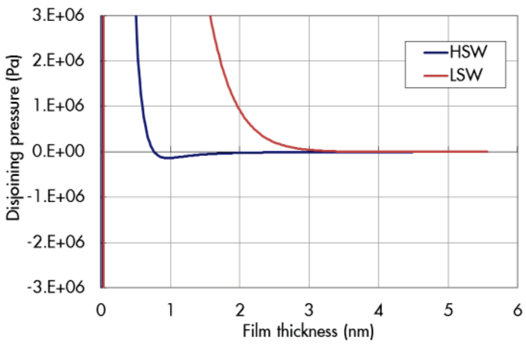

Figure 9 Disjoining pressure versus film thickness with formation brine and LSW in oil-wet rock

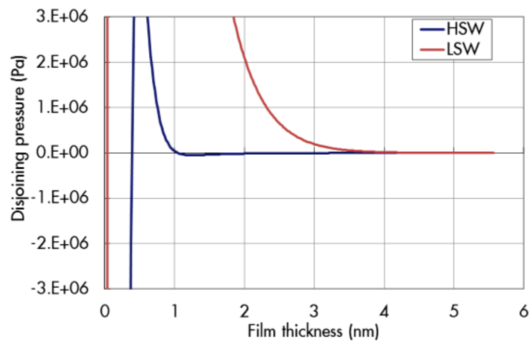

Figure 10 Disjoining pressure versus film thickness with formation brine and LSW in water-wet rock

CONCLUSION

In this study, the influence of rock wettability on the low salinity EOR-Effect was investigated by coreflood and history matching through ECLIPSE 100. Several observations were made in this study.

- Low salinity EOR-effect was observed during the low salinity waterflooding at both secondary and tertiary mode in the slightly water wet reservoir rock.
- Low salinity water can accelerate the oil production rate and decelerate the water production rate by reduction of the residual oil saturation in slightly water wet reservoirs.
- Slight wettability change and additional oil recovery were observed during the low salinity waterflood in the water-wet outcrop rock.
- Low salinity EOR-effect might be interpreted by thermodynamics of wettability. Thermodynamic calculation could help design the composition of the injection brine to enhance oil recovery.

ACKNOWLEDGEMENTS

The authors would like to thank Research Institute of Petroleum Exploration and Development of PetroChina for permission to publish this paper.

REFERENCES

1. Myint, P.C. and A. Firoozabadi, Thin liquid films in improved oil recovery from low-salinity brine. Current Opinion in Colloid & Interface Science, 2015. 20(2): p. 105-114.
2. Sheng, J.J., Critical review of low-salinity waterflooding. Journal of Petroleum Science and Engineering, 2014. 120(0): p. 216-224.

3. Sohrabi, M. and A. Emadi, Visual Investigation of Oil Recovery by Low Salinity Water Injection: Formation of Water Micro-Dispersions and Wettability Alteration, in SPE Annual Technical Conference and Exhibtion. 2013, 2013, Society of Petroleum Engineers: New Orleans, Louisiana, USA.
4. Morrow, N. and J. Buckley, Improved Oil Recovery by Low-Salinity Waterflooding. Journal of Petroleum Technology, 2011. 63(5): p. 106-112.
5. Lager, A., et al., Low Salinity Oil Recovery-An Experimental Investigation1. Petrophysics, 2008. 49(1).
6. A.Lager, K.J.W., C.J.J.Black, M.Singleton, K.S.Sorbie, Low salinity oil recovery-an experimental investigation. SCA2006-36, 2006.
7. Nasralla, R.A. and H.A. Nasr-El-Din, Double-Layer Expansion: Is It A Primary Mechanism of Improved Oil Recovery by Low-Salinity Waterflooding?, in SPE Improved Oil Recovery Symposium. 2012, Society of Petroleum Engineers: Tulsa, Oklahoma, USA.
8. Hirasaki, G.J., Wettability:fundamentals and surface forces. SPE Formation Evaluation, 1991. 6(2): p. 217-226.
9. Tang, G.-Q. and N.R. Morrow, Influence of brine composition and fines migration on crude oil/brine/rock interactions and oil recovery. Journal of Petroleum Science and Engineering, 1999. 24(2-4): p. 99-111.
10. Xie, Q., et al., Ions tuning water flooding experiments and interpretation by thermodynamics of wettability. Journal of Petroleum Science and Engineering, 2014. 124(0): p. 350-358.
11. Austad, T., A. Rezaeidoust, and T. Puntervold, Chemical Mechanism of Low Salinity Water Flooding in Sandstone Reservoirs, in SPE Improved Oil Recovery Symposium. 2010: Tulsa, Oklahoma, USA.
12. Xie Quan, H.S., Pu Wanfen, The Effects of Temperature and Acide Number of Crude Oil on the Wettability of Acid Volcanic Reservoir Rock From the Hailar Oilfield. Petroleum Science, 2010. 7: p. 93-99.
13. Masalmeh, S.K., et al., Low Salinity Flooding: Experimental Evaluation and Numerical Interpretation. 2014, International Petroleum Technology Conference.
14. Jerauld, G., et al., Modeling low-salinity waterflooding. SPE Reservoir Evaluation & Engineering, 2008. 11(6): p. 1000-1012.
15. Hirasaki, G.J., Wettability:fundamentals and surface forces. SPE Formation Evaluation, 1991c. 6(2): p. 217-226.